Variable Range Hopping (VRH) charge transport and Poole-Frenkel type conduction mechanism of polypyrrole synthesized with Chemical Oxidative Polymerization

Gowtham Balu (gowthamsona@gmail.com)
Ramakrishna Mission Vidyalaya College of Arts and Science https://orcid.org/0000-0002-9790-6540
Balasubramani v

Research Article

Keywords: Polypyrrole, conduction mechanism, charge transport properties, electrical conductivity, activation energy

Posted Date: March 25th, 2022

DOI: https://doi.org/10.21203/rs.3.rs-1476232/v1

Abstract

Polypyrrole (PPy) was prepared with various weight loadings of acetic acid (10, 30 and 50 wt.%) over chemical oxidative polymerization. The structural and electrical properties of the prepared samples were characterized by XRD and electrical analysis. The charge transport mechanism of PPy was executed by Keithley (6517B) equipment performed between a voltage of 1 to 10 V by the increment of 1 V. The current over capacitor as a role of the applied voltage was carried out from 303 to 403 K temperature range. The XRD result confirms the amorphous nature of PPy. The charge transport process of PPy was deliberated by Mott's variable-range hopping (VRH) through the conductivities and they found using various weight loadings of acetic acid. The conductivity (σ_{dc}) was found to increase with the temperature increase, which indicates the semiconducting nature and the conductivity value calculated was 10^{-9} to 10^{-7} S/cm for various weight loadings of acetic acid. The I-V study outcomes the linear behavior and the semiconducting nature of PPy, and the study was completed by the explanation of the Poole-Frenkel type conduction mechanism, ln (J) vs. T plots in PPy samples at high fields. It concludes that the comparison of theoretical field-lowering coefficients β_S and β_{PF} and the experimental field-lowering coefficients β_S and β_{PF} were correlated and the result confirms the Poole-Frenkel type conduction mechanism in PPy. The activation energy diminishes from 1.22 to 1.07 eV with an increase of acetic acid weight percentage.

1. Introduction

Electrically conducting polymers is becoming more important and plays a vital role in numerous technological applications [1, 2]. It has wide care from the research peoples because of their growing potential for high-tech applications like; rechargeable batteries, electrolytic capacitors, sensors, electrochromic devices, among others [3–5]. The charge transport in conducting polymers and their composites [6–8] possess a suitable candidate for solid state devices. Electrically conducting polymers such as polypyrrole (PPy) have nearly exclusive chemical and electrochemical possessions. PPy has viewed as per one of the most considered conducting polymers [9]. PPy is a good semiconductor and having metallic behavior, good mechanical strength, good environmental stability, higher conductivity than many other conducting polymers and low-cost easy preparation, due to these recompenses it can be used in various applications such as organic light-emitting devices [10], wires [11], gas sensors [12, 13], batteries [14, 15], biosensors [16, 17], microactuators [18], packaging, electronic devices and functional membranes, electrochromic windows and displays, etc. [19–21]. The electrical conductivity of PPy were found and reported in literature to be 10^{-6} S/cm to 10^{2} S/cm and its band gap nearly 3 eV. In PPy, polarons and bipolarons are the majority charge carriers whose sign is in control intended for their charge transport mechanism [22]. The transport mechanism in electrically conducting polymers and its composites have a boundless attention meanwhile the preparation of polyacetylene by Ito et al [23]. Subsequently, the hopping conduction mechanism is fully explained in PPy [24, 25] and the Mott's variable range hopping (VRH) model is a suitable candidate with various nature of PPy up to 403 K temperature [26]. In the present work, the structural properties, dc conductivity and the charge transport mechanism of PPy was analyzed and reported.

2. Experimental Details

2.1 Materials used for synthesis

Pyrrole purchased from Sigma-Aldrich, acetic acid, ammonium persulfate (APS), acetone, methanol from Merck, distilled water was used for the preparation of aqueous solutions.

2.2 Preparation of PPy

PPy was prepared with various amount loadings of (10, 30 and 50 wt.%) of acetic acid by chemical oxidative polymerization [27]. Pyrrole (Sigma-Aldrich) monomer was dissolved in 200 ml of distilled water with nonstop stirring for 1 h. Next step was added various amount loadings of (10, 30 and 50 wt.%) of acetic acid (Merck) to the above solution with nonstop stirring. Polymerization progression was takes place at below 5°C, by the addition of 0.1 M APS (Merck) mixed in 100 ml distilled water to the overhead solution. The polymerization progression was carried out continued stirring of 24 h at room temperature. After that, the resultant solution was several times washed with distilled water, methanol (Merck) and acetone (Merck) to remove the unwanted oligomers. The washing procedure repeated many times until the polymerization solution became colorless. The collected product was dried under vacuum oven for 24 h at 60°C to get the synthesized PPy.

The synthesized PPy powders were systematically grinded using a mortar to get a prominent particle, and they were squeezed lower than a burden of 15 torrs in the form of a pallet with a diameter of 0.6 cm, to improve the electrical contact the faces of the pellets were coated with a silver paste to dorm a parallel plate capacitor structure. The prepared product was crammed among two copper probes by pressure communication. The dc conductivity measurements of PPy remained executed by a Keithley (6517B) electrometer with a two-probe arrangement by smearing a voltage of 1 V to 10 V with collective step by step of 1 V.

3. Results And Discussion

3.1 X-Ray diffraction (XRD) Analysis

The structural properties of PPy using APS as an oxidant were characterized with XRD analysis. Figure 1 illustrates the XRD pattern of PPy (50 wt.%) executed at room temperature. The strong broad peak at 2θ = ~ 25° confirms the amorphous nature of PPy is in good agreement based the literature [22]. There are no other peaks or additional peaks are identified, which indicates the purity of the sample. Typically, the broad peak point to quick array preparation of chains. The XRD pattern of pure PPy shows the strong broad peak approximately 2θ = ~ 25.4° contains a small movement while adding various kind of dopants have studied and reported by Hemant K. Chitte et al., [29]. Also, they have analyzed the peak shift in PPy doped with chemically and electrochemically have revealed the spherical globular like structure using the dopants [30].

3.2 Electrical Conductivity

The dc conductivity measurements of PPy were prepared with various weight loadings of acetic acid (10, 30 and 50 wt.%) executed by a Keithley (6517B) electrometer with a two-probe arrangement by smearing a voltage of 1 V to 10 V with collective step by step of 1 V. The I-V characteristics of PPy were carried-out as a role of the applied voltage was carried out from 303 to 403 K temperature range. Figure 2 (a-c) depicts the I-V analysis of PPy which indicates the linear performance and confirms the ohmic transfer due on the way to the existence of updraft formed charge transporters [31]. When the impact of applied electric field, the movement of imprisoned charges in the PPy act as active dipoles [32], it pays to the development of polarons and bipolarons. When the strong point of the applied electric field increases, the grade of alteration also increased, which results the extension of current, similarly, it rises with rise in temperature. The dc conductivity was calculated using the relation [28],

$$\sigma_{DC} = \left(\frac{1}{R}\right) x \left(\frac{L}{A}\right)$$

1

where ‘R’ is the resistance, ‘L’ is the thickness, ‘A’ is the active area of the sample.

The temperature dependence of dc conductivity (σ_{dc}) of PPy were prepared with various weight loadings (10, 30 and 50 wt.%) of acetic acid between 303 to 403 K temperature as shown Fig. 3 (a-c). It illustrates that the increasing order of conductivity which confirms the semiconducting nature [33] of PPy between the temperature range 303 to 403 K. The increase of conductivity due to the polarons from one neighboring state to nearest neighboring states. The conductivity value calculated is 9.49 x 10^{-9}, 6.22 x 10^{-8} and 3.37 x 10^{-7} S/cm for 10, 30 and 50 wt.% of acetic acid (Table 1), respectively.

Table 1
DC conductivity of PPy with different weight percentage

S. No.	Sample	DC conductivity (σ_{dc}) (S/cm)
1	PPy 10wt% of acetic acid	9.49 x 10^{-9}
2	PPy 30wt% of acetic acid	6.22 x 10^{-8}
3	PPy 50wt% of acetic acid	3.37 x 10^{-7}

3.3 Hopping conduction in PPy

Mott’s variable-range hopping (VRH) [16] model gives the information about the dc conductivity is $\sigma_{dc} = \sigma_0 \exp[-(T_0/T)^x]$, where σ_{dc} is the dc conductivity, σ_0 is the pre-exponential conductivity, T_0 is the temperature that governs the thermally initiated hopping amid confined circumstances at dissimilar drives. To inspect the dimensionality of hopping conduction, the restrained dc conductivity stood examined for 1D, 2D and

3D hopping conduction besides the outcomes of dc conductivity (σ_{dc}) remained plotted against the temperature $T^{-1/2}$, $T^{-1/3}$, and $T^{-1/4}$, for 10, 30 and 50 wt.% of acetic acid. Aimed at some appropriate value of x, the plot of (σ_{dc}) versus T^{-x} should be a straight line and linearity aspect of these plots resolve the dimensionality of hopping. Consequently, the σ_{dc} versus $T^{-1/2}$, $T^{-1/3}$, and $T^{-1/4}$ were fitted for linearity. From the observed results, σ_{dc} versus $T^{-1/2}$ plot give best linear fit among $T^{-1/3}$ and $T^{-1/4}$ curve. Figure 4 shows the plot between log σ versus $T^{-1/2}$, it confirms the straight line which indicates 1D Mott's VRH model [34–36] in PPy samples.

3.4 Conduction Mechanism in PPy

Figure 5 shows typical plots of ln J against $E^{1/2}$ for the prepared PPy with various weight loadings (10, 30 and 50 wt.%) of acetic acid at different temperatures. It displays the improved linearity done the extensive series of biasing current which designates the electrical-kind conduction, moreover owing to the Schottky or the Poole-Frenkel conduction mechanism [37, 38]. To detect the particular mechanism dominant in PPy, theoretical field-lowering coefficients $\beta_{Schottky}$ and $\beta_{Poole-Frenkel}$ based on the equations (2) and (3).

$$\Delta\phi_S = e\left(\frac{e}{4\pi \in ' \in_0}\right)^{1/2} F^{1/2} = e\beta_S F^{1/2}$$

2

$$\phi_{PF} = e\left(\frac{e}{\pi \in_0 \in '}\right)^{1/2} F^{1/2} = e\beta_{PF} F^{1/2}$$

3

where m, e, k_B, φ_0 and T is the mass of the electron, electronic charge, Boltzmann's constant, interfacial barrier height and the absolute temperature. High frequency dielectric constant of the PPy with various weight loadings (10, 30 and 50 wt.%) of acetic acid attained from dielectric analysis were compared with the corresponding experimentally obtained $\beta_{experimental}$. The calculated value of $\beta_{experimental}$ from Fig. 6, the slopes between g versus e/k_BT. The $\beta_{experimental}$ and $\beta_{theoretical}$ values were illustrated in Table 2. It specifies the $\beta_{experimental}$ values are nearer to the obtained values of $\beta_{Poole-Frenkel}$ than $\beta_{Schottky}$. So, the suitable conduction mechanism in PPy samples at high fields, is Poole-Frenkel type. Rendering to this mechanism, the barricade altitude about a restricted center is lowered at high fields, so the conductivity increases due to a countless quantity of charge carriers is free from the center and improves the conductivity [39, 40]. Similar results were analyzed and reported by C.Basavaraja et al., for the electrical conduction mechanism of Polypyrrole-Alginate Polymer Films [41].

Table 2
Theoretical and experimental values of field-lowering coefficients

S. No.	Sample	Theoretical field-lowering coefficients β ($eV\ V^{1/2}\ m^{1/2} \times 10^{-5}$)		Experimental field-lowering coefficients β_{exp} ($eV\ V^{1/2}\ m^{1/2} \times 10^{-5}$)	
		β_S	β_{PF}	β_S	β_{PF}
1	PPy 10wt% of acetic acid	8.85	1.77	1.68	1.67
2	PPy 30wt% of acetic acid	8.77	1.75	1.30	1.59
3	PPy 50wt% of acetic acid	6.06	1.21	1.23	1.02

3.5 Activation Energy in PPy

The temperature dependence of dc conductivity of PPy prepared with various weight loadings of acetic acid (10, 30 and 50 wt.%) were elucidated by Arrhenius equation,

$$J = J_0 \exp\left(\frac{-E_a}{k_B T}\right)$$

4

where J_0 is the pre-exponential factor, E_a is the activation energy, k_B is the Boltzmann constant, and T is the temperature in Kelvin. The E_a was calculated from the slope of Arrhenius plot of ln J vs. 1000/T. The E_a plots of PPy prepared with various weight loadings of acetic acid (10, 30 and 50 wt.%) as shown in Fig. 7. T.K. Vishnuvardhan et al., [42] have analyzed and reported the activation energy of pure PPy were found to be 0.30 eV. In the present work the observed activation energy for PPy were shown in Table 3. It shows that the weight percentage of acetic acid was added to polymer matrix, the activation energy decreases with an increasing weight percentage of acetic acid signifying that the possible barricade is downhearted in the occurrence of an outside electric field.

Table 3
DC Activation energy of PPy with different weight percentage

S. No.	Sample	DC activation energy (E_a) (eV)
1	PPy 10wt% of acetic acid	1.22
2	PPy 30wt% of acetic acid	1.15
3	PPy 50wt% of acetic acid	1.07

Conclusion

The charge transport mechanism in these PPy was investigated by temperature-dependent dc conductivity measurements. The XRD results confirms the amorphous nature of PPy. The I-V study results confirms the linear behavior of the PPy. The temperature dependence of conductivity recommends a semiconducting behavior of PPy. 1 Dimensional charge transport mechanism in the PPy confirmed by Mott's VRH model. The Poole-Frenkel type conduction mechanism is dominating at high fields in PPy which confirmed by the experimental value of theoretical field-lowering coefficients (β) is closer to the calculated values of β_{PF}. The activation energy diminishes with an increase of acetic acid weight percentage. Based on the overhead study and report concludes that the PPy is an apt material for temperature dependent hybrid structure diodes and other optoelectronic switches.

References

1. P. Abthagir, Syed, R. Saraswathi, J. Mater. Sci.: Mater. Electron. **15**(2), 81–86 (2004)
2. S.R. Forrest, Chemical reviews 97, no. 6 (1997): 1793–1896
3. M. Kodama, J. Yamashita, Y. Soneda, H. Hatori, K. Kamegawa, Carbon **45**, 1105 (2007)
4. F. Lufrano, P. Staiti, Int. J. Electrochem. Sci. **5**, 903 (2010)
5. S. Patrice, Y. Gogotsi, Nat. Mater. **7**, 845 (2008)
6. S. Kivelson, Phys. Rev. Lett. **46**, 1344 (1981)
7. R. Singh, R.P. Tandon, V.S. Panwar, S. Chandra, J. Appl. Phys. **64**, 2504 (1991)
8. B. Gowtham, V. Ponnuswamy, V. Balasubramani, S. Ramanathan, G. Pradeesh, Ehab El Sayed Massoud, Sreedevi Gedi. Inorg. Chem. Commun. **135**, 109105 (2022)
9. M. Omastova 1993 Synth. Met. 53 227
10. A.C. Grimsdale, K.L. Chan, R.E. Martin, P.G. Jokisz, A.B. Holmes, Synthesis of lightemitting conjugated polymers for applications in electroluminescent devices. Chem. Rev. **109**, 897–1091 (2009)
11. C. Jerome, D. Labaye, I. Bodart, R. Jerome, Electrosynthesis of polyacrylic/polypyrrole composites: formation of polypyrrole wires. Synth. Met. **101**, 3–4 (1999)

12. D. Kincal, A. Kumar, A.D. Child, J.R. Reynolds, Conductivity switching in polypyrrole-coated textile fabrics as gas sensors. Synth. Met. **92**, 53–56 (1998)
13. N.T. Kemp, G.U. Fianagan, A.B. Kaiser, H.J. Trodahl, B. Chapman, A.C. Partridge, R.G. Buckley, Temperature-dependent conductivity of conducting polymers exposed to gases. Synth. Met. **101**, 434–435 (1999)
14. B. Scrosati, Conducting polymers: advanced materials for new design, rechargeable lithium batteries. Polym. Int. **47**, 50–55 (1998)
15. H.K. Song, G.T.R. Palmore, Redox-active polypyrrole: toward polymer-based batteries. Adv. Mater. **18**, 1764–1768 (2006)
16. J.C. Vidal, E. Garcia, J.R. Castillo, In situ preparation of a cholesterol biosensor: entrapment of cholesterol oxidase in an overoxidized polypyrrole film electrodeposited in a flow system: determination of total cholesterol in serum. Anal. Chim. Acta **385**, 213–222 (1999)
17. T.E. Campbell, A.J. Hodgson, G.G. Wallace, Incorporation of erythrocytes into polypyrrole to form the basis of a biosensor to screen for rhesus (D) blood groups and rhesus (D) antibodies. Electroanalysis **11**, 215–222 (1999)
18. E. Smela, Microfabrication of PPy microactuators and other conjugated polymer devices. J. Micromech Microeng **9**, 1–18 (1999)
19. T.A. Skotheim, R. Elsenbaumer, J. Reynolds (eds.), *Handbook of Conducting Polymers* (Marcel Dekker, New York, 1998)
20. G.G. Wallace, G. Spinks, P.R. Teasdale, Conductive Electroactive Polymers, Technomic, New York, 1997
21. T.A. Skotheim (ed.), *Handbook of Conducting Polymers, vols. I and II* (Marcel Dekker, New York, 1986)
22. A. Imani, G. Farzi, A. Ltaief, Int. Nano Lett. **3**(1), 1–8 (2013)
23. T. Ito, H. Shirakawa, S. Ikeda, J. Polym. Science: Polym. Chem. Ed. **12**, 11–20 (1974)
24. A. Kaur, A. Dhillon, D.K. Avasthi, J. Appl. Phys. **106**, 073715–073711 (2009)
25. R. Singh, A. Kaur, K.L. Yadav, D. Bhattacharya, Curr. Appl. Phys. **3**, 235 (2003)
26. M. Taunk, A. Kapil, S. Chand, Open. Macromol. J. **2**, 74–79 (2008)
27. B. Gowtham, V. Ponnuswamy, G. Pradeesh, R. Suresh, S. Ramanathan, S. Ashokan, J. Inorg. Organomet. Polym Mater. **30**(6), 2197–2203 (2020)
28. B. Gowtham, V. Ponnuswamy, V. Balasubramani, S. Ramanathan, G. Pradeesh, Ehab El Sayed Massoud, and Sreedevi Gedi, Inorganic Chemistry Communications (2021): 109105
29. K. Hemant, N.V. Chitte, A.V. Bhat, N. Gore, Ganesh, Shind, Mater. Sci. Appl. **2**, 1491–1498 (2011)
30. T.K. Vishnuvardhan, V.R. Kulkarni, C. Basavaraja, S.C. Raghavendra, Synthesis, Characterization and A.C. Conductivity of Polypyrrole/Y2O3 Composites. Mater. Sci. **29**(1), 77–83 (2006) “,”,
31. N.A. Hegab, H.E. Atyia, J. Ovonic Res. **2**(3), 21–29 (2006)
32. M.R. Bengoechea, F.M. Aliev, N.J. Pinto, J. Phys. Condensed Matter **14**, 11769 (2002)

33. J. Aguilar-Hernandez, K. Potje-Kamloth, J. Phys. D **34**(11), 1700 (2001)
34. N. Mott, Francis, *and Edward A. Davis. Electronic processes in non-crystalline materials* (Oxford university press, 2012)
35. A. Epstein, H. Joseph, R. Rommelmann, H.W. Bigelow, D.M. Gibson, Hoffmann, D.B. Tanner, Phys. Rev. Lett. **50**, no. 23 (1983) 1866.
36. N.F. Mott, Metal-Insulator Transition 2nd edn (London: Taylor-Francis) and references therein (1990)
37. F.H. Abd-El Kader, W.H. Osman, R.S. Hafez, Phys. B **408**, 140 (2013)
38. N. Nagaraj, Ch.V. Subba Reddy, A.K. Sharma, V.V.R. Narasimha Rao, J. Power Sources **112**, 326 (2002)
39. N.A. Hegab, H.E. Atyia, J. Ovonic Res. **2**(3), 21–29 (2006)
40. P.R.A.V.E.E.N.K. Jain, N. Saxena, J. Non-Oxide Photonic Glasses **1**, 43–52 (2009)
41. C. Basavaraja, E.A. Jo, B.S. Kim, D.G. Kim, D.S. Huh, Macromol. Res. **18**(11), 1037–1044 (2010)
42. T.K. Vishnuvardhan, V.R. Kulkarni, Int. J. Res. Eng. Technol. **02**, 554–556 (2013)

Figures

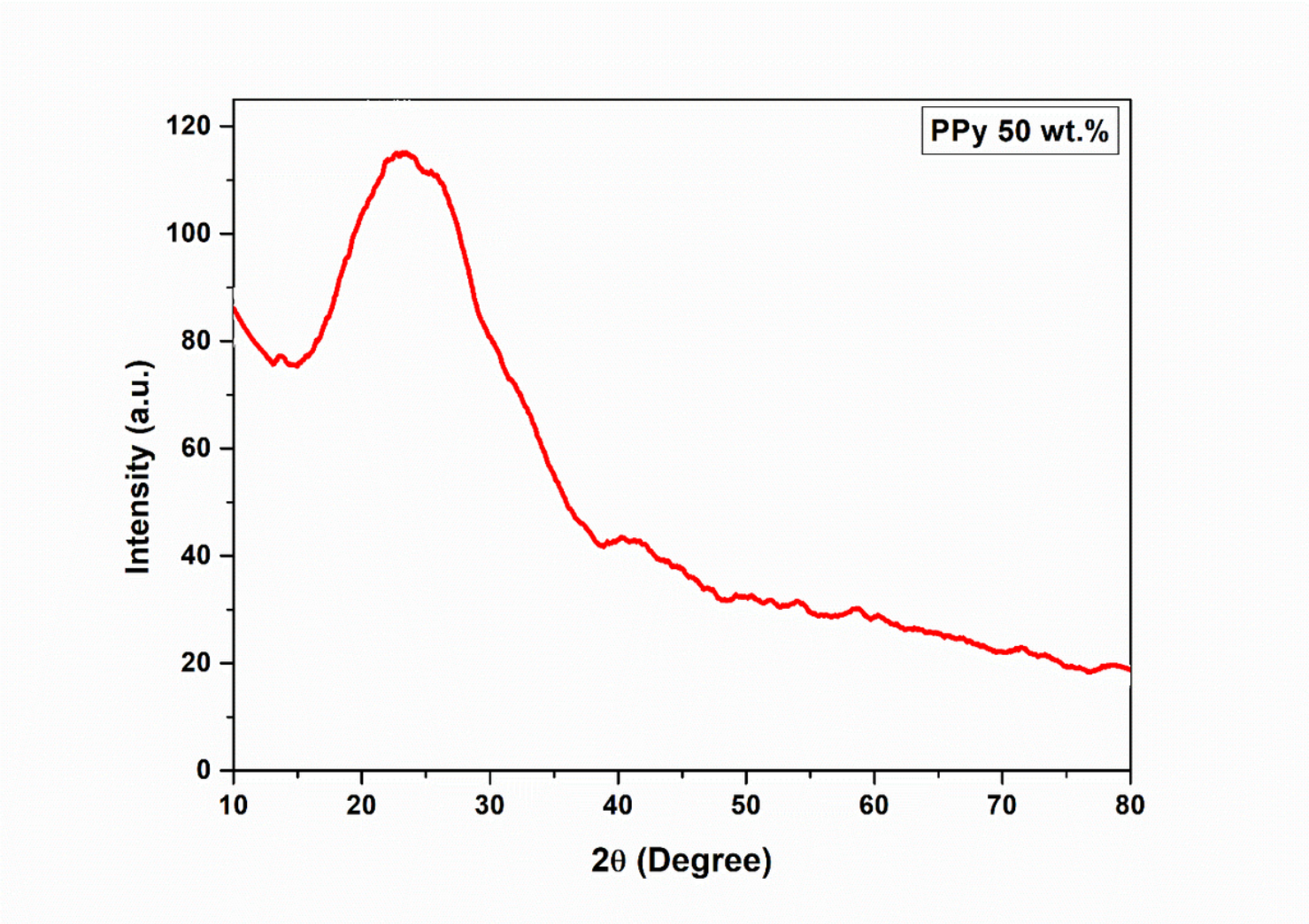

Figure 1

XRD spectrum of PPy prepared with 50 wt.% of acetic acid

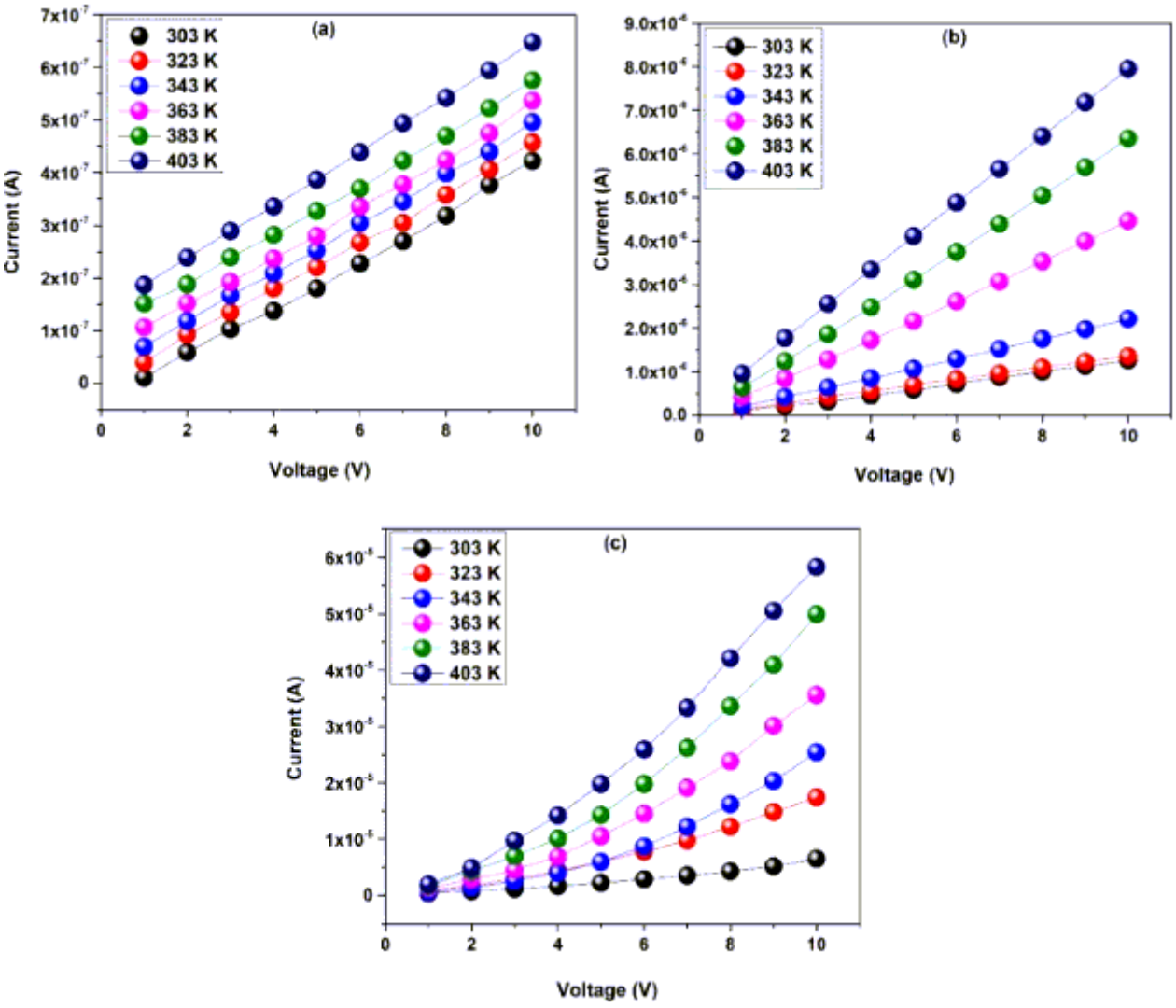

Figure 2

(a-c) I-V characteristics of PPy with different weight percentage of acetic acid 10 wt.%, 30 wt.% and 50 wt.%, respectively.

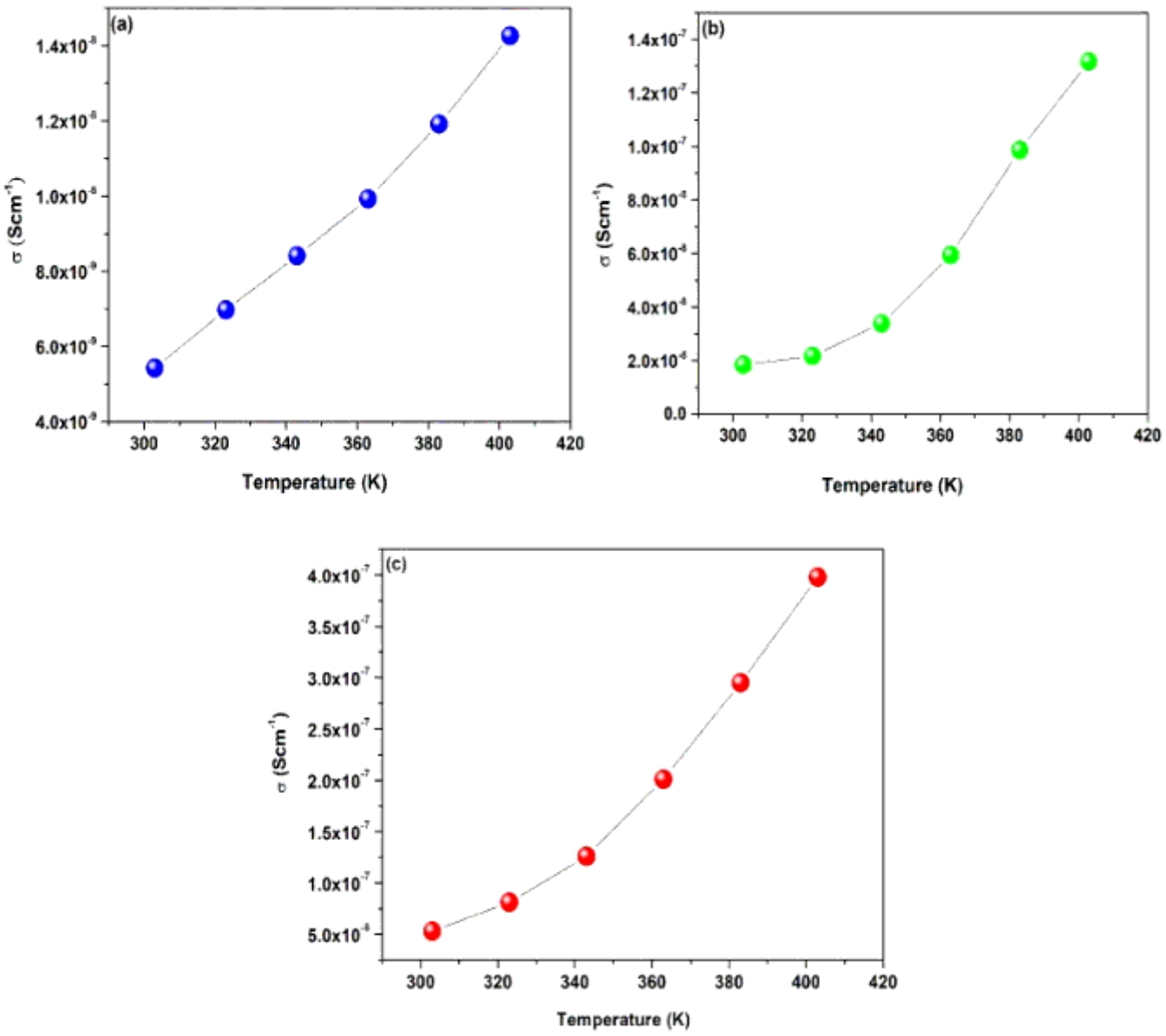

Figure 3

(a-c) The temperature dependence of DC conductivity of PPy with different weight percentage of acetic acid 10 wt.%, 30 wt.% and 50 wt.%, respectively.

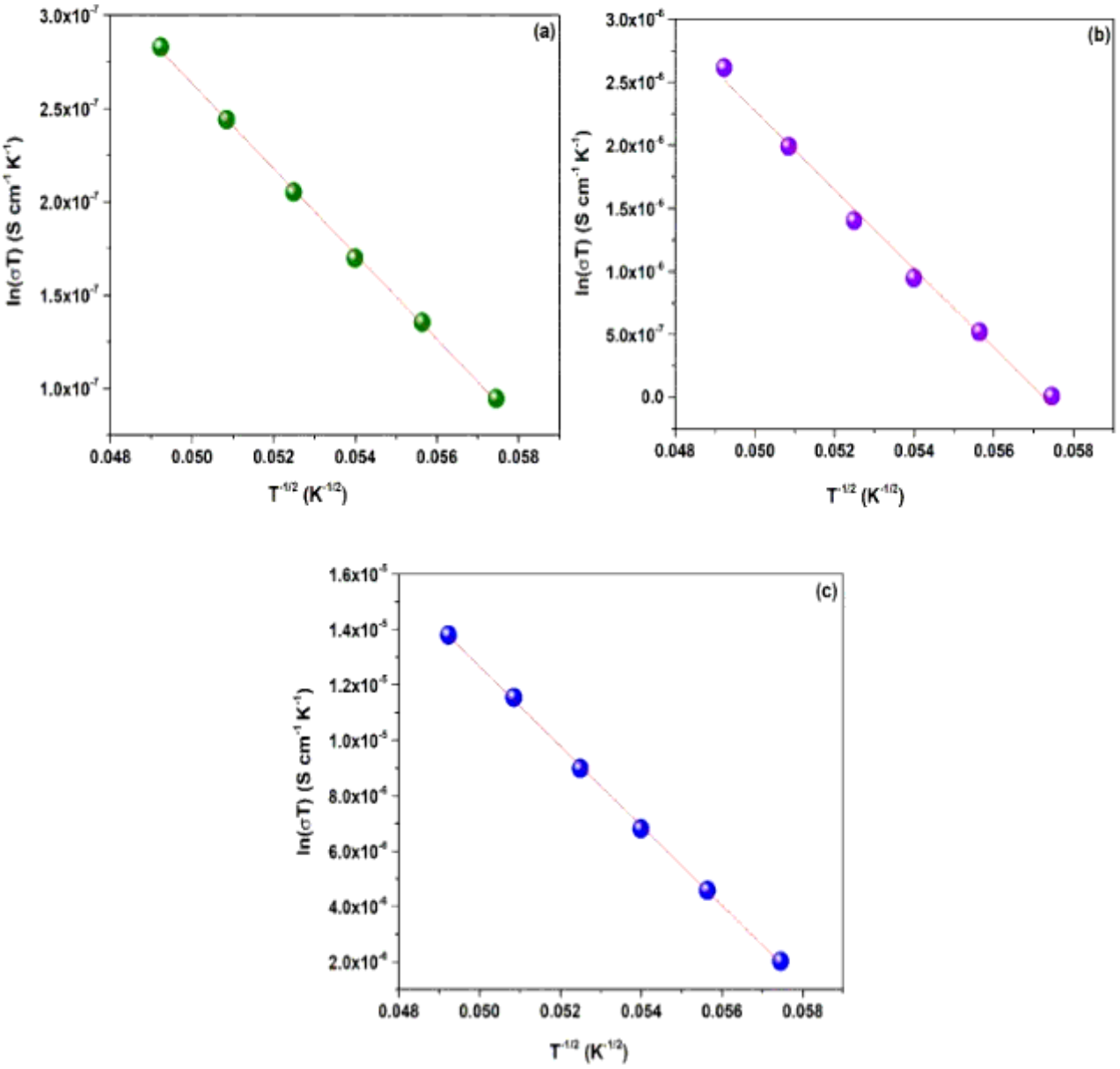

Figure 4

(a-c) Temperature dependence of dc conductivity of PPy with different weight percentage of acetic acid 10 wt.%, 30 wt.% and 50 wt.% showing a fit to 1D VRH. The solid lines are the straight-line fits obtained by the least squares fitting procedure.

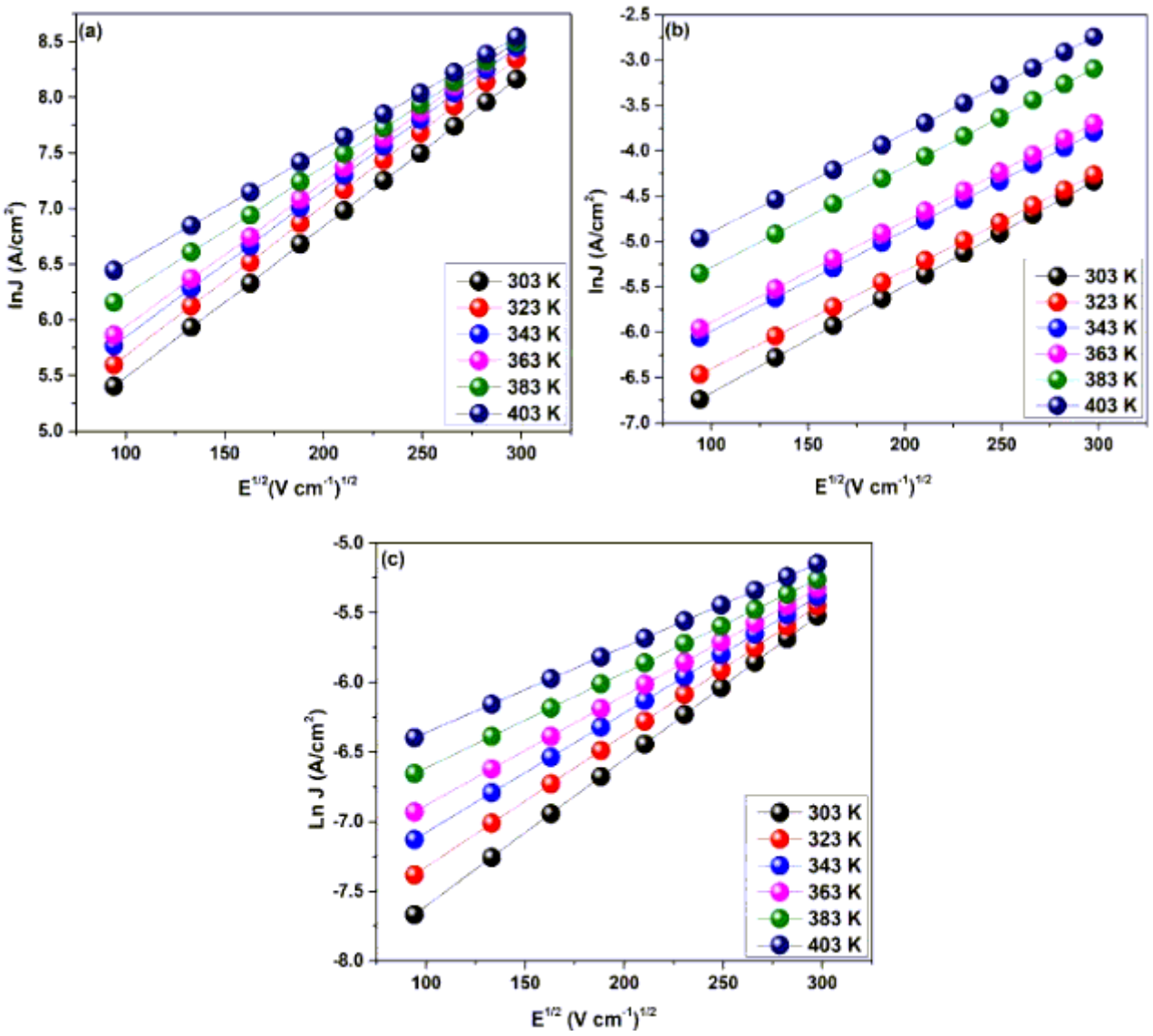

Figure 5

(a-c) Plots of ln J vs. $E^{½}$ of PPy with different weight percentage of acetic acid 10 wt.%, 30 wt.% and 50 wt.%, respectively. The solid lines are the straight-line fits obtained by the least square fitting procedure.

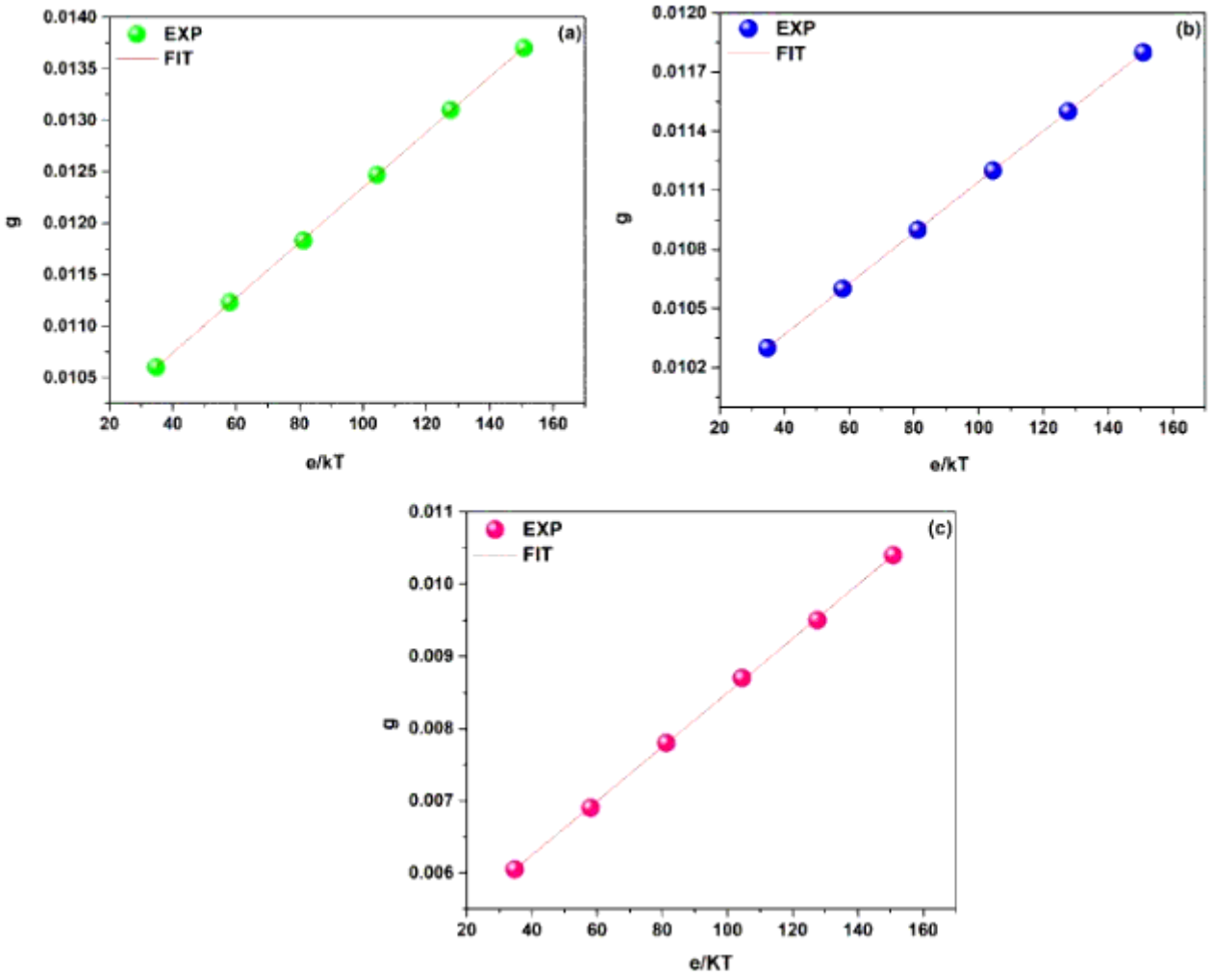

Figure 6

The slope of straight-line for the plots of g vs. e/k_BT yields the value of β_{exp} drawn by the least square fitting procedure.

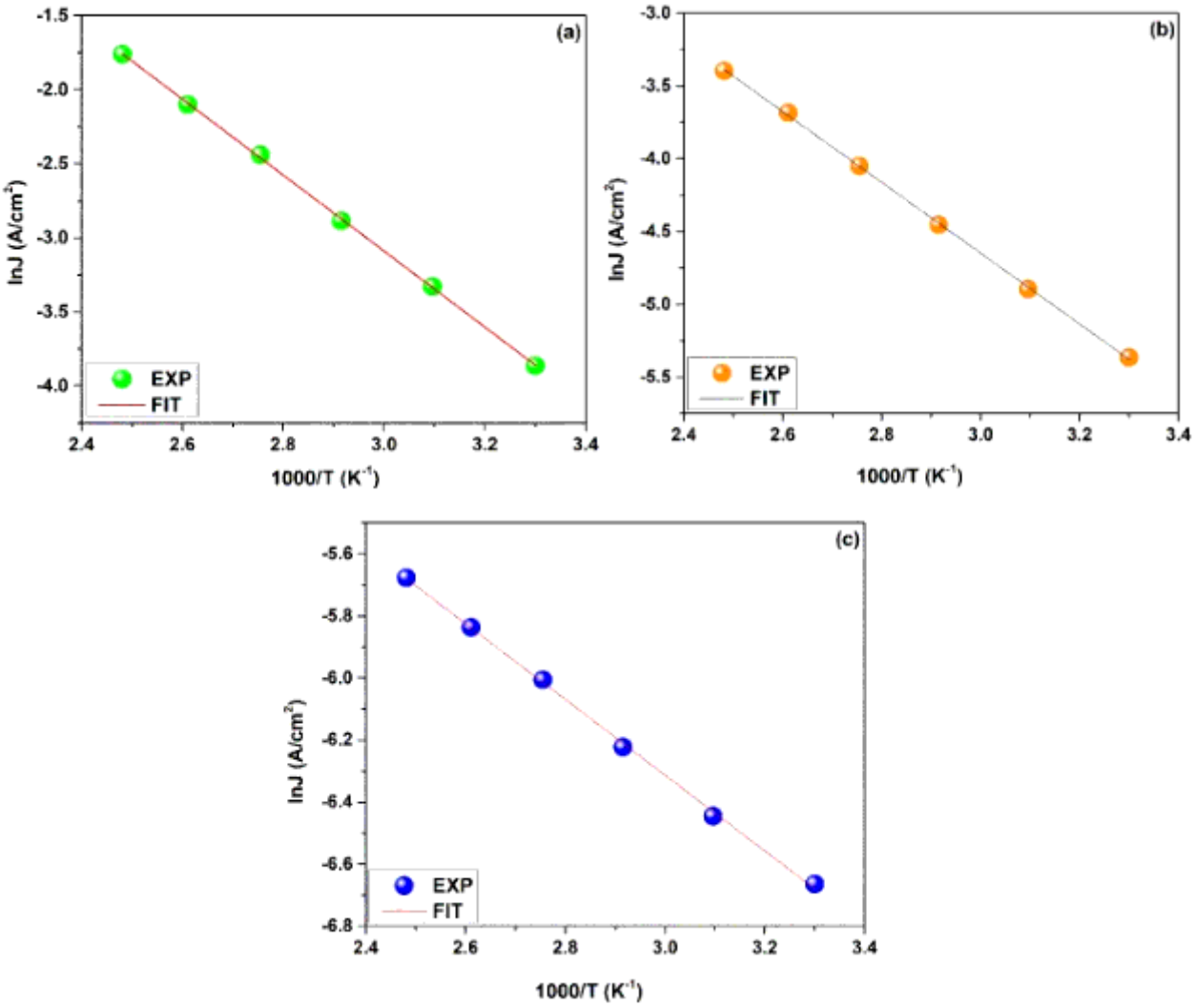

Figure 7

Plots of ln J against 1000/T for PPy with different weight percentage of acetic acid 10 wt.%, 30 wt.% and 50 wt.%, respectively. The solid line is the straight-line fits obtained by the least square fitting procedure.